ARTICLES

Synthesis and Growth of ZnO Nanoparticles

Eric A. Meulenkamp†

Philips Research Laboratories, WA 13, Prof. Holstlaan 4, 5656 AA Eindhoven, The Netherlands

Received: January 8, 1998; In Final Form: May 17, 1998

ZnO nanoparticles in the size range from 2 to 7 nm were prepared by addition of LiOH to an ethanolic zinc acetate solution. This method [Spanhel, L.; Anderson, M. A. *J. Am. Chem. Soc.* **1991**, *113*, 2826] was modified and extended at several points. The synthesis of very small ZnO nuclei was simplified. It was found that aging of particles was governed by temperature, the water content, and the presence of reaction products. Water and acetate induced considerably accelerated particle growth. Growth could almost be stopped by removal of these species ("washing"). Washing consisted of repeated precipitation of ZnO by addition of alkanes such as heptane, removal of the supernatant, and redispersion in ethanol. The aging characteristics are interpreted in terms of the concentration of dissolved Zn^{II} species and reactions well-known in sol−gel chemistry. These findings present a better-defined and more versatile procedure for production of clean ZnO sols of readily adjustable particle size. Such sols are of particular interest for studies of electrical and optical properties of ZnO nanoparticle films. For example, films exhibiting >99% transparency in the visible region could only be obtained by deposition from a washed sol.

1. Introduction

Research on nanocrystalline materials has increased enormously during the past years.[1] The intense investigations are stimulated by several envisaged application areas for this new class of materials. For example, the novel optical, electrical, and mechanical properties of devices comprising nanocrystallite semiconductors and oxides have been demonstrated in photovoltaic solar cells,[2] light-emitting diodes,[3] varistors,[4] and ceramics.[5] Other applications include ion-insertion batteries and electrochromic devices.

II−VI semiconductors such as CdSe[6] and CdS,[7] which are studied because of novel size-dependent optical and electrical properties, can be prepared with very low dispersity and accurate size control for particle sizes <50 Å. In the field of ceramic (oxidic) nanoparticles work focused on somewhat larger particles, and the effort has been geared toward production of larger quantities of material[8] and development of new synthetic routes.[9] The knowledge regarding particle synthesis and surface chemistry is not as mature as with II−VI sulfides and selenides.

This paper discusses synthesis and growth of ZnO with particle size <10 nm. ZnO is an interesting material from several points of view. It is one of the few oxides that shows quantum confinement effects[10] in an experimentally accessible size range. Investigations of such effects in nanocrystallites have been limited mostly to sulfides and selenides,[11] where they were coupled to the development of sophisticated preparation routes. However, size-dependent optical absorption is also a valuable tool to study ZnO synthesis and growth. Second, a sol−gel preparation method due to Spanhel and Anderson[12] offers a simple route to quantum size ZnO particles. Furthermore, ZnO is a technologically important material. It finds widespread use in varistors.[4] Doped ZnO is a well-known transparent conductor.[13] ZnO nanoparticles offer considerable potential as starting material for such applications and for other purposes such as transparent UV-protection films and chemical sensors.

ZnO can be considered a workhorse to get a better understanding of sol−gel synthesis and growth of oxidic nanoparticles. Recent work by other groups on nanostructured TiO_2 and Cd,Zn chalcogenides is aimed at the same goal.[14,15] The preparation of ZnO and factors that influence the rate of particle growth are studied. The results enable a more controlled and more versatile easy-to-use preparation method of (quantum size) ZnO particles for studies of for example electrical and optical properties and for their consolidation into thin films or three-dimensional solid bodies.

2. Experimental Section

Apparatus. ZnO particle size was determined by light-field transmission electron microscopy (300 kV, Philips CM30) and by analysis of the width of the X-ray diffraction (XRD) peaks according to the Debye −Scherrer equation. XRD was performed on a Philips PW 1800 diffractometer. Optical absorption spectra were recorded on a Perkin-Elmer Lambda 19 or a Unicam UV2 spectrophotometer. Separation of precipitated ZnO particles from the supernatant was done by filtration, decantation, or ultracentrifugation (Beckmann J2-21).

Chemicals. Zinc acetate dihydrate and lithium hydroxide monohydrate ($LiOH{\cdot}H_2O$) were from Aldrich. Absolute ethanol (p.A.), lithium chloride, lithium acetate dihydrate, sodium acetate, potassium acetate, glacial acetic acid, hexane, and heptane were all from Merck. All chemicals were used as received unless mentioned otherwise.

† E-mail meulenka@natlab.research.philips.com.

S1089-5647(98)00730-5 CCC: $15.00
Published on Web 06/25/1998

3. Results

3.1. Synthesis. The preparation procedure described by Spanhel and Anderson,[12] which has also been used by other groups,[16,17] was used. A few modifications were made here. A 1.10 g (5 mmol) sample of $Zn(Ac)_2 \cdot 2H_2O$ was dissolved in 50 mL of boiling ethanol at atmospheric pressure. Contrary to Spanhel and Anderson and other workers,[12,16,17] the solution was not refluxed for a few hours but directly cooled to 0 °C. A white powder precipitated close to room temperature. X-ray diffraction showed that this was anhydrous zinc acetate, $Zn(Ac)_2$. Precipitation was not observed in the original preparation procedure.[12]

A 0.29 g (7 mmol) sample of $LiOH \cdot H_2O$ was dissolved in 50 mL of ethanol at room temperature in an ultrasonic bath and cooled to 0 °C. In ref 12 the hydroxide was added in solid form to the Zn^{2+}-containing solution. However, it was found that dissolution was very slow in that case, even when aided ultrasonically. The hydroxide-containing solution was added dropwise to the $Zn(Ac)_2$ suspension under vigorous stirring at 0 °C. The reaction mixture became transparent when about 0.1 g of LiOH had been added. The ZnO sol was stored at ≤4 °C to prevent rapid particle growth.

The synthesis could be simplified further by using anhydrous zinc acetate instead of the dihydrate. $Zn(Ac)_2$ was prepared by dissolution of the dihydrate and subsequent cooling to 0 °C. The precipitate was filtered off, washed with ethanol, and dried. Addition of the hydroxide-containing solution to the appropriate amount of finely ground $Zn(Ac)_2$ powder under the conditions outlined above resulted in a transparent ZnO sol, similar to that prepared from zinc acetate dihydrate.

The concentration of water in the reaction mixture was found to be of paramount importance. Karl Fischer titration of a standard ZnO sol showed a ±1.2 vol % water content. This originates from ethanol, hydrated salts (±0.2 vol %), adsorbed water on powder reactants, and water produced by the chemical reaction between Zn^{2+} and OH^- (±0.1 vol %). A "dry" synthesis was carried out for comparison using molsieves-dried ethanol and chemicals dried under 0.3 atm at 120 °C. The water content of the "dry" ZnO sol was ±0.5 vol %. Similar results were obtained as with the standard method except for much slower dissolution of the reactants and slower growth of ZnO particles. When 1.0 vol % of water was added to the standard reaction mixture ("wet" synthesis), no ZnO was formed. Hence, the presence of a small, but strictly limited, quantity of water appeared necessary to warrant a successful synthesis.

3.2. Precipitation and Redispersion. *Washing.* Since this work aims to study particle growth, it was considered important to find a method to remove reaction products (LiAc and H_2O) from the ZnO sol. Hoyer and co-workers[16] achieved this by precipitation of ZnO aggregates through addition of water, washing of the precipitate with cold ethanol, and redispersion in ethanol. This procedure was also effective in the present case, but two drawbacks became apparent. The washed sol was often somewhat turbid (optical transmission at 400 nm ≈ 95% for twice-concentrated ZnO), suggesting that complete disagglomeration after precipitation was not possible. Second, water plays an important role in growth of ZnO particles (see below), and addition can, therefore, lead to unwanted side effects.

It was found that precipitation can also be effected by addition of an organic "nonsolvent". This is well-known for CdSe and CdS nanocrystallites[6,7] but has, to the best of our knowledge, not been reported for ZnO. Hydrocarbons with long alkane chains, such as hexane and heptane, were particularly suitable. Heptane is preferable because it is less toxic. Typically, the required volume ratio of hexane/heptane to ZnO sol was between 1:1 and 2:1. The supernatant was removed by decantation or centrifugation. The ZnO precipitate was redispersed in ethanol. This procedure could be repeated several times. The ionic conductivity of the original ZnO sol was about 500 μS cm^{-1}. After one and two washing steps this was reduced to approximately 50 and ≲10 μS cm^{-1}, respectively.

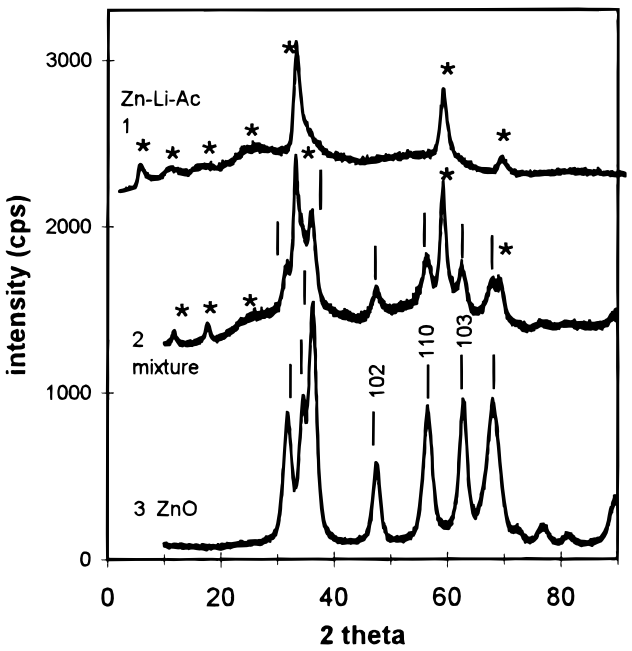

Figure 1. Powder X-ray diffraction (XRD) patterns of precipitates obtained by addition of heptane to ZnO sols after various periods of aging. Curves have been offset for the sake of clarity. Curve 1 shows the basic zinc−lithium−acetate obtained within 1 day after synthesis. Peaks are labeled (*). Curve 2 shows the precipitate obtained after approximately 1 day. ZnO peaks are labeled (|). Curve 3 represents pure nanocrystalline wurtzite ZnO. The reflection peaks used for particle size determination (see section 3.3) are labeled *hkl*.

The effective removal of unwanted ionic species was confirmed by chemical analysis of ZnO films spin-coated from the twice-washed solution. Films were heated to 150 °C for 10 min to remove the solvent. (Anderson and co-workers[18] have shown that this does not lead to removal of acetate, if present.) Li was determined by ICP-OES and acetate by ion chromatography. A Li/Zn atomic ratio <0.004 and an acetate/Zn atomic ratio <0.0013 were found. The maximum ratios were determined by the detection limits.

Basic Zinc−Lithium−Acetate. Attempts to precipitate very small ZnO particles led to unexpected results. Hexane was added to a ZnO sol (kept at ≤0 °C) within 1 day after preparation, and the mixture was kept at low temperature until a white powder precipitated. This required several hours. Ion chromatography, ICP-OES, and acid titration identified the material as a basic zinc−lithium−acetate. This is consistent with zinc(II) chemistry. For example, basic zinc acetate, with chemical formula $Zn_4O(Ac)_6$ or $ZnO.3Zn(Ac)_2$, is well-known.[19] Evidence for the presence of zinc−lithium−acetate complexes in acetic acid has also been reported.[20] Spanhel and Anderson[12] mentioned a detailed investigation of an organometallic zinc precursor containing acetic acid derivatives, but this work has not been published as far as we are aware. More recent work[15] has identified the precursor as $Zn_{10}O_4(Ac)_{12}$, the next-higher homologue of $Zn_4O(Ac)_6$.

Figure 1 shows diffraction patterns for the basic zinc−lithium−acetate (curve 1, peaks marked "*"). Note the peak

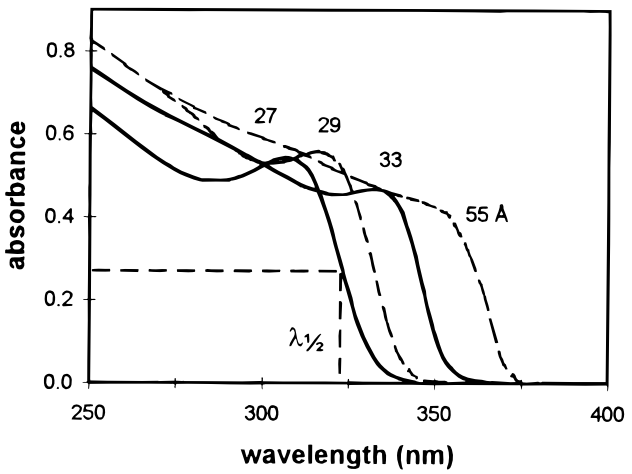

Figure 2. UV/vis absorbance spectra of ZnO sols. Dashed lines show the procedure to determine $\lambda_{1/2}$ for a particle sizes of 27 Å. The indicated particle size is obtained from the fit shown in Figure 3 (solid line).

at small 2θ (±6°). The diffractogram was compared with standard powder diffraction patterns of $Zn_4O(Ac)_6$ and of phases containing Zn, Li, O, OH, or Ac but could not be identified. The Zn/Ac ratio was about 2.0. It was observed that the peak positions and their relative intensities changed slightly with time under ambient conditions. A detailed elucidation of the structure and composition was not attempted. Curve 3 shows the XRD pattern of pure nanocrystalline ZnO (peaks marked "|") which was precipitated approximately 1 week after synthesis. The broadening of the ZnO peaks is due to the small particle size. Curve 2 is the diffractogram of a precipitate that contained both materials.

The gradual transition of the composition of the precipitate from the basic zinc−lithium−acetate to pure ZnO shows that conversion of the precursor to ZnO nanocrystallites is very slow. This was confirmed by synthesis in a cuvette at 0 °C inside a spectrophotometer. The characteristic ZnO band gap absorption (see below) was not observed until after several hours, in accordance with previous work.[21] The importance of the zinc−lithium−acetate compound and the precursor for the present work is that they highlight complexation of zinc in acetate-containing solutions.

Size Selective Precipitation. During washing it was noted that precipitation of smaller particles required larger volumes of hexane/heptane. Therefore, size selective precipitation of ZnO nanoparticles was attempted. This process has up to now only be described for sulfides and selenides[6,7] where it represents a useful way to decrease polydispersity. However, careful heptane addition under various experimental conditions did not give rise to a significantly decreased polydispersity of either the supernatant or the precipitate. The optical absorption spectra of the precipitate and the supernatant were almost identical. Precipitation by addition of water gave similar results.

3.3. Particle Size Determination. ZnO shows quantum size effects for particles $\lesssim$7 nm.[10] Hence, UV/vis absorbance spectra provide a convenient way to investigate particle growth. Optical absorption spectra for ZnO sols are presented in Figure 2. Various ways have been used to determine the band gap E_g from such measurements.[10,12,16,17,21,22] A practical method is to equate E_g with the wavelength at which the absorption is 50% of that at the excitonic peak (or shoulder), called $\lambda_{1/2}$. This is schematically shown in Figure 2. This graphical procedure also allowed calculation of E_g from UV/vis spectra published by other workers. $\lambda_{1/2}$ and the inflection point calculated by differentiation were within 1 nm for almost all samples studied.

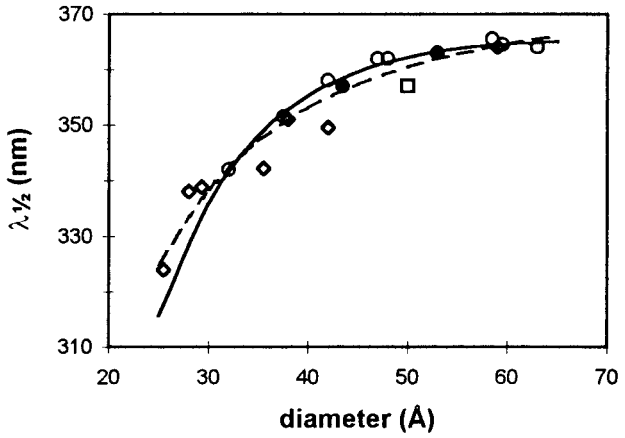

Figure 3. Size dependence of the optical band gap, defined as $\lambda_{1/2}$. Open symbols refer to TEM results and closed symbols to XRD size determinations. Data shown are by Hoyer and co-workers[14] (◇), from ref 21 (□), and from the present work (○, ●). Fits according to the expression $1240/\lambda_{1/2} = a + b/D^2 - c/D$ are shown as a solid line (present data) and as a dashed line (all data).

Particle size was determined from TEM micrographs and XRD line broadening. To a good approximation, UV/vis and XRD measurements provide volume-weighted averages. (The oscillator strength for the first exciton absorption did not show a large dependence on particle diameter; the scatter factor for XRD is independent of particle size *d*.[23]) A size histogram was used to calculate this quantity from TEM micrographs.

In Figure 3 all data relating particle size and band gap are collected. Open symbols refer to TEM experiments and closed symbols to XRD results. The agreement between data by Weller and co-workers (◇)[16] and the present work is excellent. Note that XRD (●) and TEM (○) results of the present work are in good agreement. This was also found in ref 12. Thus, we conclude that either method gives reliable results. Other workers (□) have also reported (sets of) data relating size and optical band gap.[10,12,17,22] These have, for the greater part, not been included in Figure 3 because they were mostly obtained for ZnO prepared by different routes or because recalculation of $\lambda_{1/2}$ was not possible. Figure 3 is used below to analyze the evolution of particle size during aging. We have also used it to study the effect of particle size on the ZnO dissolution rate[24] upon addition of acid. The lines in Figure 3 represent fits to an expression[32] of the form $1240/\lambda_{1/2} = a + b/D^2 - c/D$ ($\lambda_{1/2}$ in nm, diameter D in Å). If only the present results (solid line) are used, $a = 3.556$, $b = 799.9$, and $c = 22.64$. A fit of all data points yields $a = 3.301$, $b = 294.0$, and $c = -1.09$ (dashed line). Both give a good description of the experimentally found size dependence for $25 < D < 65$ Å and are used below to convert measured values of $\lambda_{1/2}$ into particle size.

It was checked that $\lambda_{1/2}$ was not affected by ion adsorption or small changes of the solution composition. Agglomeration can also influence the optical properties by electronic interaction between contacting particles. Only sols showing no or negligible light scattering were used. TEM micrographs of such samples confirmed the absence of agglomeration. Hence, UV/vis data presented can be interpreted in terms of the *primary* particle size throughout this work.

3.4. Particle Growth. ZnO nanoparticles continue to grow, or *age*, after synthesis, even when stored at 0 °C. The ability to obtain various particle sizes is based on this phenomenon. It was found that the solution composition and temperature have a marked influence on the rate of particle growth. Figure 4

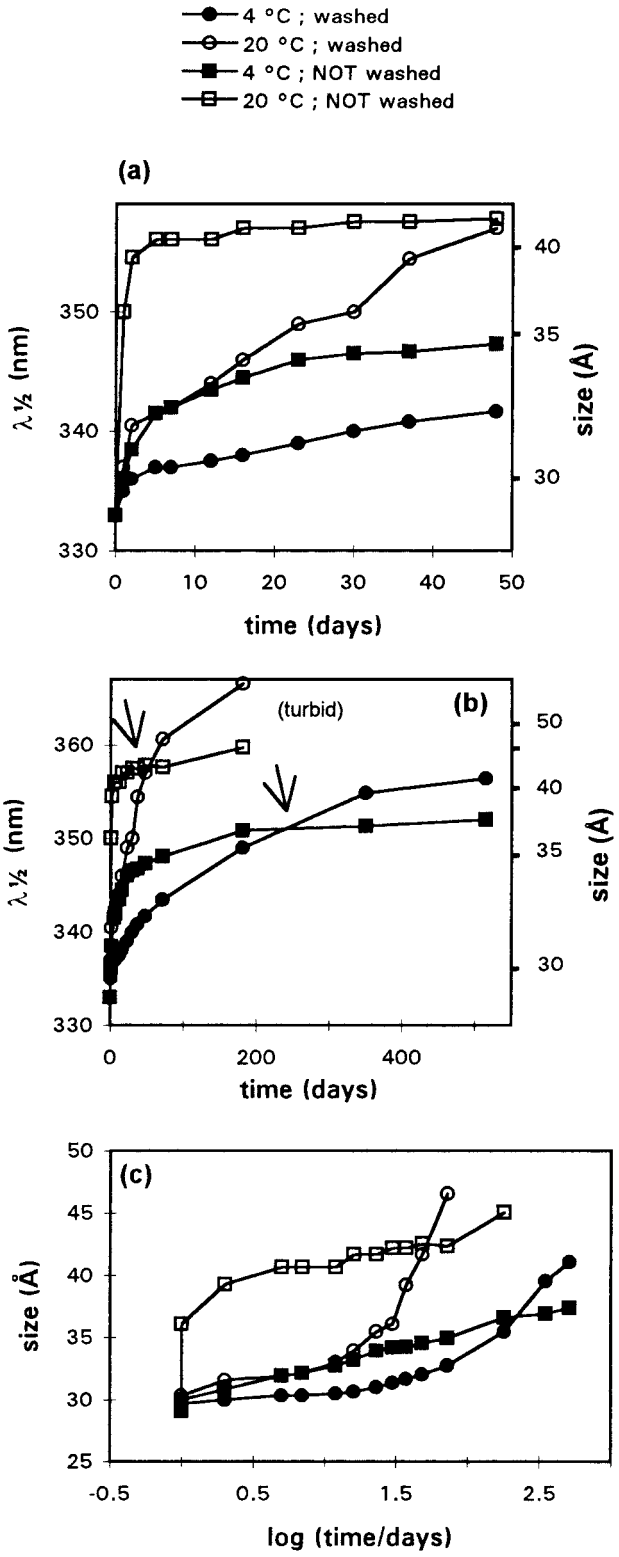

Figure 4. Evolution of $\lambda_{1/2}$ of ZnO sols during aging under various conditions: (●) washed and aged at 4 °C, (○) washed and aged at 20 °C, (■) original sol aged at 4 °C, and (□) original sol aged at 20 °C. (a) shows data during the early stages of aging. (b) shows all data. The same data have been converted into particle size (using the fit through the present results shown as a solid line in Figure 3) vs logarithm of time in (c).

shows the evolution of $\lambda_{1/2}$ and size for ZnO sols subjected to different treatments. A sol was prepared and divided in two parts after 1 week to avoid precipitation of the basic zinc−lithium−acetate. One part was washed and redispersed in ethanol (circles); the other part was not treated (squares). Both fractions were split and stored at 4 °C (●, ■) or room temperature (○, □). The final ZnO concentration of all fractions was similar. Figure 4a emphasizes the development during the early stages of aging. Figure 4b shows the results for prolonged storage. The same data, given as particle size vs the logarithm of time, are presented in Figure 4c.

The data given by closed symbols and corresponding open symbols in Figure 4a can be compared to study the effect of temperature. Growth was markedly accelerated when particles were kept at room temperature (RT, ≈20 °C), as expected. Comparison of samples stored at the same temperature is more interesting: washed sols (circles) showed far slower growth than untreated sols (squares). For example, $\lambda_{1/2}$ of the untreated sol stored at RT was about 356 nm (41 Å diameter) after 5 days; this should be compared to the washed fraction stored at RT with $\lambda_{1/2} = 342$ nm (32 Å diameter). This fraction reached a 41 Å particle size only after ±45 days. The degree of polydispersity, as estimated from the sharpness of the excitonic absorption peak, was similar for both samples at a given particle size. It should also be noted that the washed sol showed almost no particle growth during a brief period of time (day two to six).

Inspection of Figure 4b revealed another intriguing feature. Washed sols showed (much) smaller particle sizes than their unwashed counterparts during the early stages of aging. This situation was reversed after prolonged storage. The arrows indicate the "crossover" that occurred after about 55 days and about 240 days at RT and 4 °C, respectively. It is concluded that particles in a washed sol show slower particle growth which, however, continues for a longer time. The RT sols showed turbidity after approximately 200 days, and the experiment was stopped. Slow agglomeration was typical of sols with $\lambda_{1/2} \gtrsim 360-365$ nm.

Figure 4c displays the type of data that can be obtained on the basis of the calibration graph of size vs band gap (Figure 3). Note the logarithmic time axis. There is a marked difference between growth of washed sols and untreated sols. The latter show a dependence of particle size D on time t which can be described as $D = a \log t +$ constant, with $a \approx 2.5$. Remarkably, a was the same for both temperatures studied. The particle size of washed sols increased approximately linearly with time, for $t < 100$ days.

Such (D,t) relationships seem not to have been studied intensively, except for the case of SiO_2,[25] where it was shown that they depend on the kinetics of aging. For example, the rate of particle growth is inversely proportional to particle size if a surface reaction (e.g., dissolution) is the rate-limiting step. If the growth rate is determined by incorporation of solute species in already existing particles, it can be expected to be proportional to the concentration of that solute species. Iler[26] has also discussed various models for the rates of particle dissolution and growth. However, the relationships observed here could not be explained on the basis of such models. The kinetics of particle dissolution are discussed in more detail in ref 24.

Washing removes several reactants and reaction products. It was, therefore, decided to investigate the effect of those species separately. In a typical experiment, various concentrations of salts were added to a fresh (washed or untreated) ZnO sol, and the $\lambda_{1/2}$ values were determined during several weeks. The final ZnO concentration of all samples was identical. A reference sample (no additional species added) was also studied.

Figure 5 shows some results for an untreated sol. Acetic

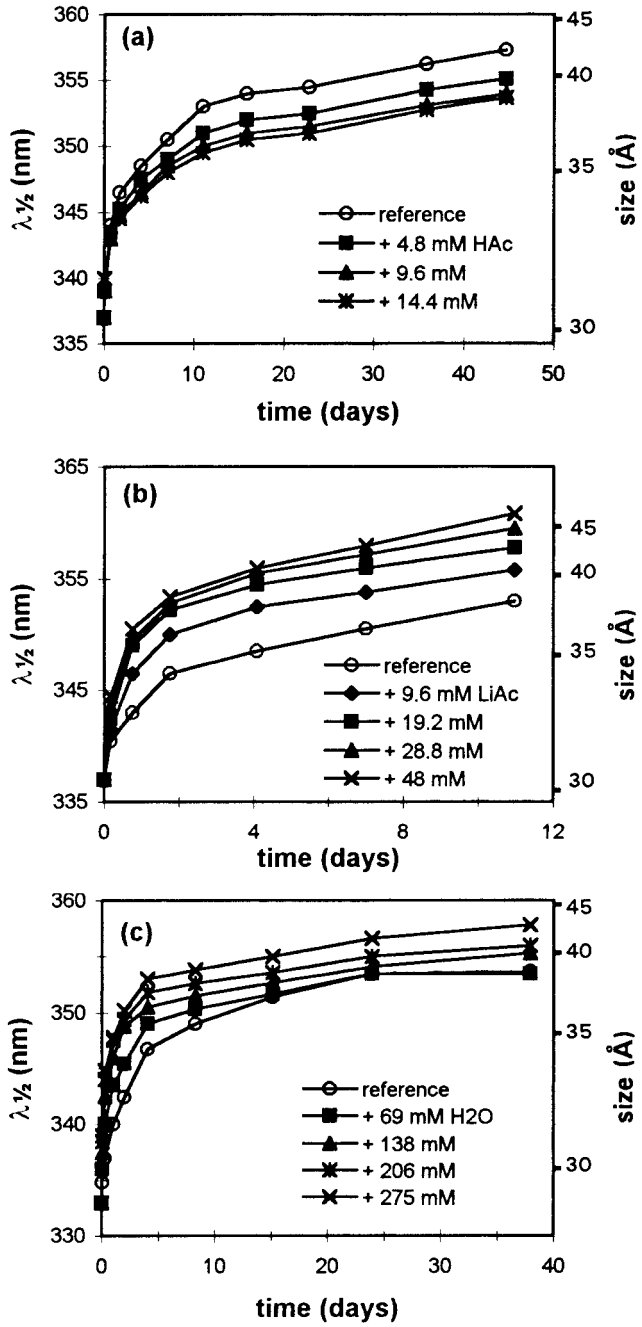

Figure 5. Effect of solution composition on the rate of ZnO particle growth (unwashed dispersions), shown as the optical band gap $\lambda_{1/2}$. The final concentrations of additives are indicated in the figures. (a) and (b) show addition of HAc and LiAc·$2H_2O$, respectively. The final ZnO concentration of all samples was equivalent to 20 mM Zn(II); (c) shows addition of H_2O to a "dry" (see section 2.1) ZnO sol. The final ZnO concentration of all samples was equivalent to 7 mM Zn(II); the added concentration of water is indicated in the figure.

acid (Figure 5a) induced slower growth. All other species led to faster aging. LiAc·$2H_2O$ is shown as a typical example in Figure 5b. After 1 week the reference sample and that with 48 mM LiAc added showed particle sizes of about 36 and 42 Å, respectively. It was found that addition of LiCl accelerated particle growth to the same extent. The influence of water was studied by using a "dry" ZnO sol (see section 3.1) because agglomeration took place upon addition of water to a standard ZnO sol. The results are collected in Figure 5c. Water accelerated particle growth. This can be seen, for example, by comparing $\lambda_{1/2}$ of the reference curve (○) with that showing addition of 275 mM H_2O (×).

The effects of the individual species can be appreciated by comparison of the results outlined in Figure 5a−c and by some additional experiments. The role of water is already clear. The effect of hydrated LiAc (Figure 5b) can then be due to the addition of water, acetate, and lithium ions. The addition of anhydrous NaAc or KAc also accelerated particle growth. Comparison of the effects of LiAc, NaAc, and KAc at the same water content did not show a significant cation effect. The effect of MAc (M = Li, Na, K) is therefore ascribed to acetate.The addition of hydrated LiAc results in the combined effects of water and acetate. Indeed, addition of 28.8 mM LiAc·$2H_2O$ (58 mM H_2O) led to much faster particle growth than addition of 69 mM H_2O. Glacial acetic acid (Figure 5a) retarded particle growth. Hence, a pH decrease has a profound effect on aging. This is not unexpected because part of the ZnO dissolved, and a much lower ZnO content was obtained. A small increase of pH (LiOH addition) had a larger effect than addition of the same amount of HAc, and considerably faster particle aging was observed.

Similar results were found when salts or water were added to a washed ZnO sol. Thus, it is concluded that removal of water and acetate is responsible for the marked effect of washing which was described above and depicted in Figure 4.

4. Discussion

4.1. Preparation and Handling. The present work uses a preparation procedure that was modified at several points compared to earlier work. It is important to assess whether the properties of the nanoparticles obtained differ in any respect. The calibration plot of size vs band gap (Figure 3) showed that results by Weller and co-workers agree well with the present data. Comparison of the optical absorption spectra, in particular the presence of an excitonic peak, and TEM size histograms points out that the degree of polydispersity is also similar. (Here, 85−90% of the particles have a size within 20% of the mean diameter.) Electrochemical characterization of films spin-coated on ITO[27] revealed that the potential of the onset of electron accumulation and, hence, surface charge were almost identical to that described by Hoyer and Weller.[14,28] Luminescence excitation and emission spectra (not shown) were similar to those reported by Spanhel and Anderson. It is, therefore, concluded that no significant differences exist between ZnO nanoparticles prepared by the original method[12,16] and by the modified, less time-consuming procedure outlined in section 2.1.

Some effort was dedicated to workup and handling of ZnO particles. Removal of reaction products by washing is of particular importance in this respect. Preparation of particles usually represents only the first step toward device fabrication. Chemically pure layers, or layers with well-defined chemical composition, are often required. More fundamental studies of, for example, optical and electrical properties of films can also benefit from the use of washed sols. For example, transparent films, which did not show light scattering (transmission at $\lambda >$ 380 nm >99.5%), could only be produced at a relatively low anneal temperature (≤150 °C) by using the thoroughly washed sols. Such films are essential to perform quantitative studies of, for example, the index of refraction, electrochromic effects,[16,17,24] photocurrent efficiencies,[28,29] etc., because accurate correction for scattered light intensity is very complicated if not impossible.

4.2. Particle Growth. Particle growth in colloidal systems can be viewed from two standpoints. In the classical picture, it corresponds to a decrease of the surface free energy at a constant total volume. This process is known as Ostwald

ripening: large particles grow at the expense of smaller particles, which have a higher solubility S according to the so-called Ostwald−Freundlich equation. This relation is derived from thermodynamic equilibrium considerations and does, therefore, not provide information on the *rate* at which particles grow, which is the prime interest here.

The other picture describes growth by the addition of reactive precursors available in solution to already existing particles. For the case of silica (see ref 25 for a review), extensive investigations have shown that *growth* proceeds by a surface reaction-limited condensation of precursors. Particle *nucleation* is a more complicated process, and aggregation of building units appears to occur.[30] A similar mechanism was invoked for the preparation of very small II−VI semiconductor colloids.[15]

The *rate* of particle growth is governed by the concentration of precursors or dissolved species and their reactivity, which depends on the number of particle surface atoms, and the solution composition. Here, the precursor is probably $Zn_{10}O_4(Ac)_{12}$ during the nucleation.[15] The nature of the dissolved species during continued growth is not known. Note, in this respect, that growth also takes place in a washed sol which has been redispersed from a pure ZnO precipitate. However, as complexation of Zn^{2+} by acetate is likely to occur, the dissolved species is denoted as Zn−OAc. Oxides can be formed by hydrolysis (1) and condensation (2) of the dissolved species. Hydrolysis of ZnO is equivalent to ZnO dissolution (3):[31]

$$\mathrm{Zn{-}OAc + HOH/OH^- \rightleftarrows Zn{-}OH + HOAc/OAc^-} \quad (1)$$

$$\mathrm{Zn{-}OH + Zn{-}OAc \rightleftarrows Zn{-}O{-}Zn + HOAc} \quad (2)$$

$$\mathrm{Zn{-}O{-}Zn + HOH \rightarrow Zn{-}OH + Zn{-}OH} \quad (3)$$

The effects of various additives on ZnO aging can now be interpreted in a qualitative manner as follows. Acetate (and chloride) are good complexants for Zn^{II}. They effectively increase the steady-state concentration of the dissolved species. It is well-known that the pH has a strong effect on the kinetics of the sol−gel reactions described by eqs 1−3. For example, a higher pH induces faster condensation, and vice versa, in accordance with the higher growth rate. The role of water can be manifold. It can increase the concentration of dissolved Zn^{II} species as zinc salts are generally more soluble in water than in ethanol. It also enhances the activity of all species. Thus, ZnO particle growth can be described by taking into account the known solution chemistry and condensation reactions. Similar arguments have been used to account for aging processes in SiO_2 sols and gels.[26] The effects of pH, temperature, and salts on the polymerization and neck formation between particles were ascribed to changes in the rates of dissolution/reprecipitation of monomeric silica, i.e., the dissolved species. As an example, addition of OH^- or HF resulted in faster aging.

It should be noted, however, that more complicated behavior has also been described for the case of nanostructured TiO_2.[14] The role of pH can also be more complex than outlined above, since it affects both hydrolysis (dissolution) and condensation. Additional measurements (e.g., conductivity, pH, IR, and NMR) are necessary to obtain a complete picture of the reactions and dissolved species involved in ZnO particle growth.

Finally, a brief discussion is presented of the observation that a washed sol shows a smaller particle size during the early stage of aging, but a bigger particle size after a certain time (see Figure 4b). The "final" particle size cannot be predicted in the present picture. However, it can be speculated what parameters are responsible for the observed behavior. The growth rate is assumed to be governed by the product of the concentration of the dissolved species and the surface reactivity of the ZnO particles. In a washed sol, the concentration is lower. It is possible that, at a given size, the surface reactivity is higher than in the case of an unwashed sol. The reason for this is the surface chemistry of the ZnO species. If specific adsorption takes place, as is well-known in the colloid chemical literature, the rates of reactions 1−3 can be affected. Thus, it is conceivable that growth in a washed solution continues at a measurable rate for a longer time and, therefore, that bigger particles are finally obtained.

5. Conclusions

The known method for preparation of ZnO nanoparticles in alcoholic solutions has been modified and extended. The synthetic procedure was made less time-consuming than previously reported without significant changes in various properties of ZnO particles produced. A "washing" procedure based on repeated precipitation by addition of alkanes and redispersion in ethanol was developed. The resultant sol is very useful for studies of electrical and optical properties of ZnO nanoparticle films because the chemical composition thereof is better defined and because films thus made show excellent transparency. Control of the particle size was improved by recognizing the influence of temperature, water, and reaction products (LiAc) during the aging of ZnO sols. The marked variations of the particle growth rate observed under various experimental conditions could be rationalized in terms of kinetically limited growth. The rate is governed by hydrolysis and condensation reactions well-known in the field of sol−gel chemistry and the concentration of the dissolved Zn^{II} species.

Acknowledgment. I would like to thank S. van der Putten, N. Haex, H. Wondergem, and A. Staals (Philips Research) for structural and chemical characterization of ZnO particles and films.

References and Notes

(1) See e.g.: *Nanomaterials: Synthesis, Properties and Applications;* Edelstein, A. S., Cammarata, R. C., Eds. Institute of Physics Publishing: Bristol, 1996.
(2) O'Regan, B.; Grätzel, M. *Nature* **1991**, *353*, 737.
(3) Colvin, V. L.; Schlamp, M. C.; Alivisatos, A. P. *Nature* **1994**, *370*, 354.
(4) Gupta, T. K. *J. Am. Ceram. Soc.* **1990**, *73*, 1817 and references therein. Lee, J.; Hwang, J.-H.; Mashek, J. J.; Mason, T. O.; Miller, A. E.; Siegel, R. W. *J. Mater. Res.* **1995**, *10*, 2295.
(5) See e.g.: Mayo, M.-J.; Chen, D.-J.; Hague, D. C. In ref 1, Chapter 8.
(6) Murray, C. B.; Norris, D. J.; Bawendi, M. G. *J. Am. Chem. Soc.* **1993**, *115*, 8706.
(7) Vossmeyer, T.; Katsikas, L.; Giersig, M.; Popovic, I. G.; Diesner, K.; Chemseddine, A.; Eychmüller, A.; Weller, H. *J. Phys. Chem.* **1994**, *98*, 7665.
(8) Siegel, R. W. *Mater. Sci. Eng. A* **1993**, *168*, 189.
(9) See e.g.: Chow, G. M.; Gonsalves, K. E. In ref 1, Chapter 3.
(10) Koch, U.; Fojtik, A.; Weller, H.; Henglein, A. *Chem. Phys. Lett.* **1985**, *122*, 507.
(11) Steigerwald, M. L.; Brus, L. E. *Acc. Chem. Res.* **1990**, *23*, 183.
(12) Spanhel, L.; Anderson, M. A. *J. Am. Chem. Soc.* **1991**, *113*, 2826.
(13) See e.g.: Chopra, K. L.; Major, S.; Pandya, D. K. *Thin Solid Films* **1983**, *102*, 1.
(14) Moritz, T.; Reiss, J.; Diesner, K.; Su, D.; Chemseddine, A. *J. Phys. Chem. B* **1997**, *101*, 8052.
(15) Schmidt, T.; Müller, G.; Spanhel, L.; Kerkel, K.; Forchel, A. *Chem. Mater.* **1998**, *10*, 65. Ptatschek, V.; Schmidt, T.; Lerch, M.; Müller, G.; Spanhel, L.; Emmerling, A.; Fricke, J.; Foitzik, A. H.; Langer, E. *Ber. Bunsen-Ges. Phys. Chem.* **1998**, *102*, 85.
(16) Hoyer, P.; Weller, H. *Chem. Phys. Lett.* **1994**, *221*, 379. Hoyer, P.; Eichberger, R.; Weller, H. *Ber. Bunsen-Ges. Chem. Phys. Chem.* **1993**, *97*, 630.

(17) Redmond, G.; O'Keeffe, A.; Burgess, C.; MacHale, C.; Fitzmaurice, D. *J. Phys. Chem.* **1993**, *97*, 11081.

(18) Sakohara, S.; Tickanen, L. D.; Anderson, M. A. *J. Phys. Chem.* **1992**, *96*, 11086.

(19) Hiltunen, L.; Leskelä, M.; Mäkelä, M.; Niinistö, L. *Acta Chem. Scand., Ser.* **1987**, *A41*, 548. Kunkely, H.; Vogler, A. *J. Chem. Soc., Chem. Commun.* **1990**, 1204.

(20) Griswold, E.; van Horne, W. *J. Am. Chem. Soc.* **1945**, *67*, 763.

(21) Bahnemann, D. W.; Kormann, C.; Hoffmann, M. R. *J. Phys. Chem.* **1987**, *91*, 3789.

(22) Haase, M.; Weller, H.; Henglein, A. *J. Phys. Chem.* **1988**, *92*, 482.

(23) See e.g.: Weissmüller, J. In ref 1, Chapter 10.

(24) Meulenkamp, E. A., submitted to *J. Phys. Chem. B.*

(25) See e.g.: van Blaaderen, A.; van Geest, J.; Vrij, A. *J. Colloid. Interface Sci.* **1992**, *154*, 481.

(26) Iler, R. K. *The Chemistry of Silica—Solubility, Polymerization, Colloid and Surface Properties, and Biochemistry*; John Wiley & Sons: New York, 1979.

(27) Meulenkamp, E. A. To be published.

(28) Hoyer, P.; Weller, H. *J. Phys. Chem.* **1995**, *99*, 14096.

(29) Rensmo, H.; Keis, K.; Lindström, H.; Södergren, S.; Solbrand, A.; Hagfeldt, A.; Lindquist, S.-E.; Wang, L. N.; Muhammed, M. *J. Phys. Chem. B* **1997**, *101*, 2598.

(30) Boukari, H.; Lin, J. S.; Harris, M. T. *Chem. Mater.* **1997**, *9*, 2376.

(31) Brinker, C. J.; Scherer, G. W. *Sol−Gel Science*; Academic Press: San Diego, 1990.

(32) Although this expression is identical to that used by Steigerwald and Brus[11] to calculate the size dependence of the optical band gap, the values *a*, *b*, and *c* have no physical relevance for ZnO. The inadequacy of this expression to predict quantum size effects in the case of ZnO was also noted in ref 22.